

## Optical and electrical characterizations of nanocomposite film of titania adsorbed onto oxidized multiwalled carbon nanotubes

This article has been downloaded from IOPscience. Please scroll down to see the full text article.

2005 J. Phys.: Condens. Matter 17 4361

(<http://iopscience.iop.org/0953-8984/17/27/011>)

View [the table of contents for this issue](#), or go to the [journal homepage](#) for more

Download details:

IP Address: 129.252.86.83

The article was downloaded on 28/05/2010 at 05:14

Please note that [terms and conditions apply](#).

# Optical and electrical characterizations of nanocomposite film of titania adsorbed onto oxidized multiwalled carbon nanotubes

Wei Feng<sup>1,3</sup>, Yiyu Feng<sup>1</sup>, Zigang Wu<sup>1</sup>, Akihiko Fujii<sup>2</sup>, Masanori Ozaki<sup>2</sup> and Katsumi Yoshino<sup>2</sup>

<sup>1</sup> Department of Polymer Materials Science and Engineering, School of Materials Science and Engineering, Tianjin University, Tianjin 300072, People's Republic of China

<sup>2</sup> Department of Electronic Engineering, Graduate School of Engineering, Osaka University, 2-1 Yamada-Oka, Suita, Osaka 565-0871, Japan

E-mail: [lf@xjtu.edu.cn](mailto:lf@xjtu.edu.cn)

Received 17 January 2005, in final form 18 May 2005

Published 24 June 2005

Online at [stacks.iop.org/JPhysCM/17/4361](http://stacks.iop.org/JPhysCM/17/4361)

## Abstract

Composite film containing titania electrostatically linked to oxidized multiwalled carbon nanotubes (TiO<sub>2</sub>-s-MWNTs) was prepared from a suspension of TiO<sub>2</sub> nanoparticles in soluble carbon nanotubes. The structure of the film was analysed principally by Fourier transform infrared spectroscopy, scanning electron micrography and x-ray diffraction. The optical and electrical characterizations of the film were investigated by UV–vis spectrum, photoluminescence and photoconductivity. The enhancement of photocurrent in the TiO<sub>2</sub>-s-MWNT film is discussed by taking the photoinduced charge transfer between the MWNT and TiO<sub>2</sub> into consideration.

(Some figures in this article are in colour only in the electronic version)

## 1. Introduction

Polymer-based photovoltaics are growing areas of research that hold promise for the creation of low-cost flexible devices for civilian applications. In particular, conjugated polymer-based solar cells could offer many advantages in fabrication, such as low-cost roll-to-roll production of large-area flexible solar cells. Because of these advantages, the development of polymer solar cells is supposed to have a major impact [1, 2]. However, the poor photo-induced charge separation and transport of photogenerated charges in many conjugated polymers are considered responsible for the low efficiencies of energy conversion [3].

The discovery of photo-induced electron transfer in composites of conducting polymers as donors and organic molecules as acceptors has provided a molecular approach to highly

<sup>3</sup> Author to whom any correspondence should be addressed.

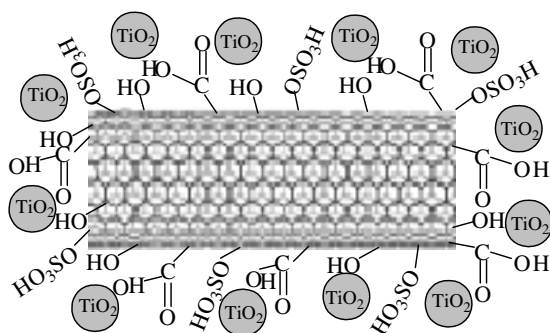


**Figure 1.** Schematic diagram of  $\text{TiO}_2$ -s-MWNT molecule.

efficient photovoltaic conversion [4–6]. It has been shown that composites of p-conjugated polymers and  $\text{C}_{60}$  have promise for application in photovoltaic devices, owing to efficient electron transfer from the conjugated polymer to  $\text{C}_{60}$  under visible light. In this respect, recently several efficient photovoltaic systems using a combination of polymer and carbon nanotube have been fabricated and demonstrated that the photovoltaic effect can be significantly improved upon the introduction of single-wall carbon nanotubes as the electron acceptors. The photovoltaic properties are due to the introduction of internal polymer/nanotube junctions within the polymer matrix. The high electric field at these junctions can split up the excitons, while the SWNTs can act as a pathway for the electrons [7, 8].

Dye-sensitized nano-crystalline solar cells are currently under intensive investigation, as they offer an alternative to conventional p–n junction devices [9, 10]. In these devices, the high power conversion efficiencies are attributable to the ultra-fast charge transfer from the dye to the  $\text{TiO}_2$ , the high surface area of the  $\text{TiO}_2$  film, the broad absorption of the dye and the efficient separation of opposite charge into different materials.

In light of the above, composite films of  $\text{TiO}_2$  and carbon nanotubes are of great interest in terms of the novel electronic interaction between these two elements and the electron transfer in the polymer solar cells [11, 12]. There have been several different recent techniques used to coat carbon supports for specific applications.  $\text{TiO}_2$  as anatase has been deposited by the sol–gel method on a multiwall carbon nanotube surface for photocatalytic application [13, 14]. Fitzmaurice *et al* [15] succeeded in depositing titanium dioxide and silica nanoparticles on the modified MWNTs by templated assembly. Kim *et al* [16] and Kovtyukhova *et al* [17] incorporated functionalized carbon nanotubes with  $\text{TiO}_2$  particles in order to improve the photovoltaic characteristics. Being a large bandgap semiconductor ( $E_g = 3.2$  eV),  $\text{TiO}_2$  has been shown to participate in the surface photochemical processes resulting in the oxidation of the adsorbed substrate. This implies that a carbon nanotube may act as a sensitizer when it attaches to the surface of  $\text{TiO}_2$ . Due to this effect, there will be photo-induced charge transfer from carbon nanotubes to  $\text{TiO}_2$ .

In this study, we report the preparation of a composite film of titania electrostatically linked to an oxidized multiwalled carbon nanotube ( $\text{TiO}_2$ -s-MWNT) by a suspension of  $\text{TiO}_2$  nanoparticles in soluble carbon nanotubes (figure 1). The structure of the film was analysed principally by Fourier transform infrared spectroscopy (FTIR), scanning electron microscopy (SEM) and x-ray diffraction (XRD). The optical and electrical characterizations of the film were investigated by UV–vis spectrum, photoluminescence (PL) and photoconductivity. Such composites are expected to be useful for applications as diverse as molecular electronics, photocatalysis, and solar energy conversion.

## 2. Experimental details

### 2.1. Materials

Titania nanoparticles (P-25) were obtained from Degussa AG, Frankfurt, in the form of 30% rutile and 70% anatase, with an average particle size of approximately 21 nm and surface area of 50 m<sup>2</sup> g<sup>-1</sup>. s-MWNT was synthesized according to the method already described in [18] and Poly(3-hexylthiophene) (PAT6) was synthesized and purified as previously reported [19]. All other solvents and chemicals were analytical reagent grade.

### 2.2. Fabrication of TiO<sub>2</sub>-s-MWNT composite film

Nanocrystalline TiO<sub>2</sub> powder, 2.4 g, was ground in a porcelain mortar with 0.8 ml water containing HNO<sub>3</sub> (0.08 ml) to prevent reaggregation of the particles. After the powder had been dispersed by the high shear forces in the viscous paste, it was diluted by slow addition of s-MWNT aqueous solution (0.4 g l<sup>-1</sup>) of 3.2 ml under continued grinding. Finally, 0.04 ml of polyethylene glycon was added to facilitate the spreading of the colloid. The colloid was applied on the patterned ITO coated glass substrate with a sheet resistance of 10 Ω/ by spin-coating. After air drying, the film was fired for 30 min at 470 °C in air. The thickness of the TiO<sub>2</sub> film was 4–6 μm.

### 2.3. Fabrication of photovoltaic device

PAT6 of an appropriate weight ratio was dissolved in chloroform. TiO<sub>2</sub>-s-MWNT film was heated at 120 °C and soaked in the PAT6 solution for 48 h. PAT6-coated TiO<sub>2</sub>-s-MWNT film was rinsed in chloroform and then dried under vacuum followed by deposition of an Al contact layer by thermal evaporation in vacuum through the shadow mask. The active area of the device is 1 × 1 mm<sup>2</sup>.

### 2.4. Characterization

Observations of titanium oxide films were performed using a Hitachi S-2100A scanning electron microscope (SEM). Fourier transform infrared spectroscopy (FTIR, JASCO corporation FT/IR-300E measurement) was used to characterize s-MWNT and TiO<sub>2</sub>-s-MWNT film. Film thickness measurements of the two kinds of titanium oxide film were carried out with AFM (JSTM-4200A scanning probe microscope). Absorption was measured using a Hitachi 330 UV-vis spectrophotometer. The photoluminescence (PL) spectra were measured by using a fluorescence spectrophotometer (F-4500, Hitachi). Photoelectrical measurements were carried out in a vacuum optical cryostat in a vacuum of about 10<sup>-5</sup> Torr. Current-voltage characteristics were measured using a Keithley 617 picoammeter. A high-intensity xenon lamp (500 W) was used as a UV-visible light source. The spectral response of the device was corrected for the response of the lamp-monochromator system by measuring the calibration spectrum with a UV-enhanced Si photodiode placed in the sample position.

## 3. Results and discussion

It is well known that when two sols of opposite sign are mixed mutual adsorption may occur [20]. Titania particles will be adsorbed onto an s-MWNT by electrostatic forces. An s-MWNT made by attaching sulfated, carboxylic acid and hydroxyl groups onto the surfaces of an MWNT has good solubility in water and a negatively charged surface, while the titania

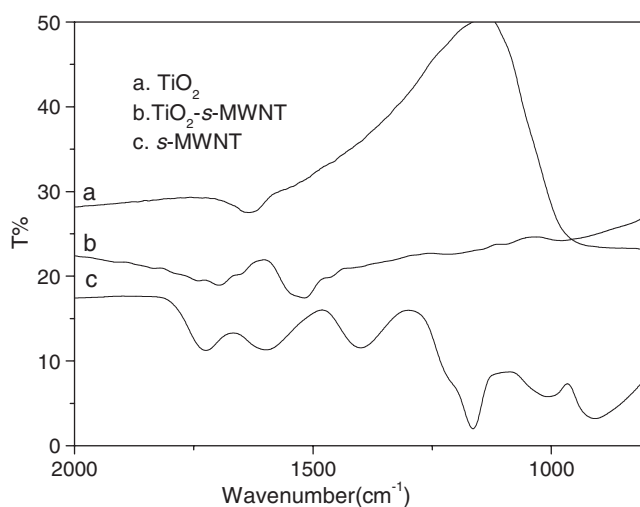


**Figure 2.** FTIR spectra of  $\text{TiO}_2$  (a), s-MWNT (b) and  $\text{TiO}_2$ -s-MWNT (c).

nanoparticles made by mixing into water with a small amount of nitric acid solution have a positively charged surface. The surface charge of titania particles is positive and they easily adsorb onto the negatively charged surface of the s-MWNT and form nanocomposites.

FTIR spectra were employed to characterize the film. Figure 2 shows FTIR spectra of  $\text{TiO}_2$ , s-MWNT and  $\text{TiO}_2$ -s-MWNT, respectively. The adsorption band at  $1635\text{ cm}^{-1}$  is attributed to the bending vibration of H–O–H bonds, which is assigned to the chemisorbed water on  $\text{TiO}_2$  in the FTIR spectrum of  $\text{TiO}_2$  (figure 2(a)), which is in good agreement with the available reference [21]. The presence of bands at (i)  $1725\text{ cm}^{-1}$ , (ii)  $1600\text{ cm}^{-1}$  and (iii)  $1003$ ,  $1168$  and  $1390\text{ cm}^{-1}$  can be attributed to (i) the stretching vibrations of C=O carboxylic moieties; (ii) aromatic ring vibrations and (iii)  $-\text{SO}_3\text{H}$  groups in the spectrum of s-MWNT (figure 2(c)) [18, 22]. Compared with the FTIR spectrum of the s-MWNT, the vibrational frequency of the C=O double bond in the  $\text{TiO}_2$ -s-MWNT spectrum (figure 2(b)) downshifts from  $1725$  to  $1695\text{ cm}^{-1}$  and this peak is weak and broad, which implies the linkage between the s-MWNT and  $\text{TiO}_2$ . Moreover, the sulfated bond region in the spectrum of  $\text{TiO}_2$ -s-MWNT film manifests greatly weak and broadened peaks comparing with that of s-MWNT, which suggests that most of the sulfated bonds contribute to the joining of the s-MWNT with titania. The above information leads us to believe that at least some of the bonding may occur through an additional ionic interaction, since recent studies have shown that acidic ions can be anchored on the surface of  $\text{TiO}_2$  [23].

Scanning electron microscopy (SEM) images revealed the  $\text{TiO}_2$ -s-MWNT sizes of and the nature of association between the  $\text{TiO}_2$  and s-MWNT (see figure 3).

For comparison, an SEM image of the original s-MWNT is also shown in figure 3. Figure 3 a shows clearly that the diameters of the s-MWNTs are in the range of 20–30 nm with a smooth surface. SEM examination verified that the s-MWNT was completely coated with nanometre titania under high shearing strength. It is obvious that carbon nanotubes are wrapped or covered by titania particles homogeneously like a layer as shown in figure 3(b). Numbers of nanocrystals tended to disperse along the sidewalls, presumably attaching to defect sites on the oxidized nanotube surface. Analysis of the nanocomposite tube surface (figure 3(b)) shows that the  $\text{TiO}_2$ -s-MWNT has a rough surface with average nanocomposite size of 50–70 nm owing to the wrapping of titania, which suggests that the s-MWNT is closely packed by titania

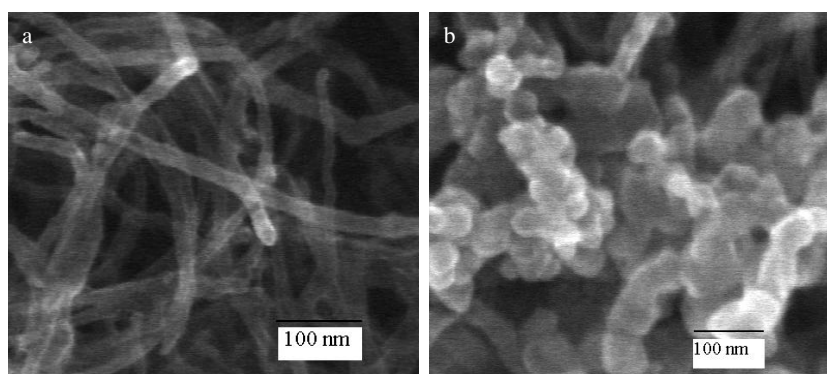


Figure 3. SEM images of the s-MWNT and the TiO<sub>2</sub>-s-MWNT films.

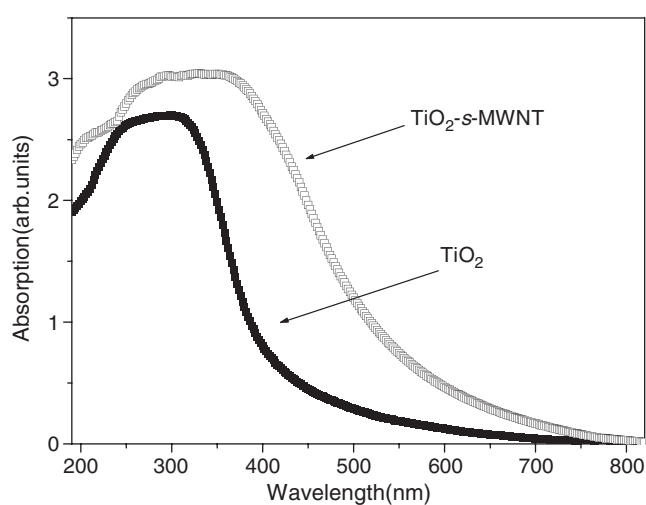
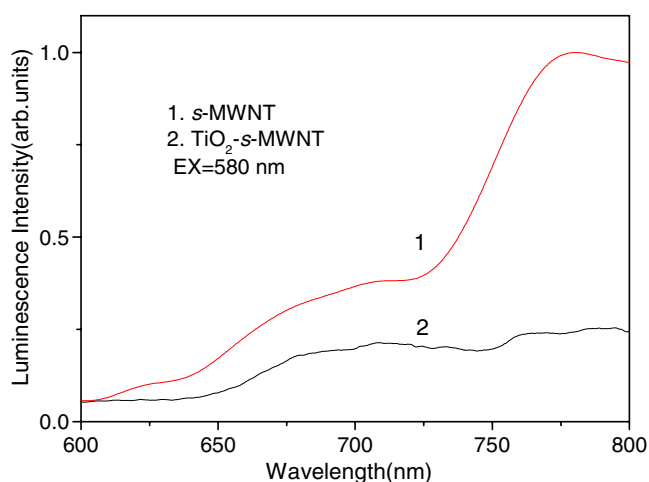


Figure 4. UV-vis absorption spectra of TiO<sub>2</sub> and TiO<sub>2</sub>-s-MWNT film.

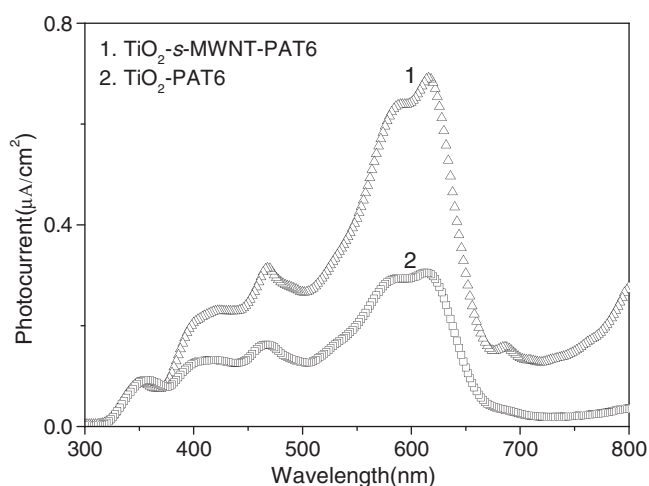
and forms a three-dimensional network of interconnected nanocomposites by the spin-coating process.

Figure 4 shows the absorption spectra of TiO<sub>2</sub> and TiO<sub>2</sub>-s-MWNT films. The spectrum of TiO<sub>2</sub> is typical for anatase, whose fundamental absorption edge is at 380 nm, corresponding to a bandgap of 3.2 eV. The TiO<sub>2</sub>-s-MWNT film produces a red shift in the absorption. This effect is particularly pronounced for the s-MWNT, where the tail of the band reaches far into the visible, and the onset is at 600 nm. The peak of optical features was also somewhat broadened in the TiO<sub>2</sub>-s-MWNT film. This indicates that the band in the visible observed in the presence of s-MWNTs corresponds to a charge transfer transition. Light promotes electron transfer from the surface of the s-MWNT to the conduction band of TiO<sub>2</sub>. Such a band should red shift with decreasing ionization potential of the electron donor as is observed in figure 4, thereby suggesting that charge separation has been achieved.

The PL spectra of s-MWNT and TiO<sub>2</sub>-s-MWNT films are shown in figure 5. As TiO<sub>2</sub> has no PL in the measured region, the PL observed should be due to the contribution of the s-MWNT. For the sake of comparison, the PL spectrum of s-MWNTs is also indicated in the



**Figure 5.** Photoluminescence spectra of s-MWNT and TiO<sub>2</sub>-s-MWNT film.



**Figure 6.** Photocurrent spectra of the devices ITO/TiO<sub>2</sub>-PAT6/Al and ITO/TiO<sub>2</sub>-s-MWNT-PAT6/Al.

same figure. It is well known that a shortened carbon nanotube is more luminescent because carbon nanotubes are considerably larger species and consist of defects (and cutting sites in shortened nanotubes). The luminescence could be due to the trapping of excitation energy at defect sites [24]. As evident in this figure, the s-MWNT has a large PL peak at 770 nm with a shoulder at 700 nm. However, the PL intensity of the TiO<sub>2</sub>-s-MWNT film is significantly quenched compared with that of the s-MWNT film. The PL quenching efficiency is about 75%. This suggests that electron transfer from s-MWNT to TiO<sub>2</sub> is occurring and that the charge transfer is fast enough to compete with the radiative recombination of excitons in the s-MWNT. These results indicate that  $\pi$ -electron delocalization increases with TiO<sub>2</sub> attaching onto the sidewall of the s-MWNT.

Usually in the composite system of conjugated polymer and carbon nanotube, the carbon nanotube acts as electron acceptor and transport path [25]. However, s-MWNTs may be able

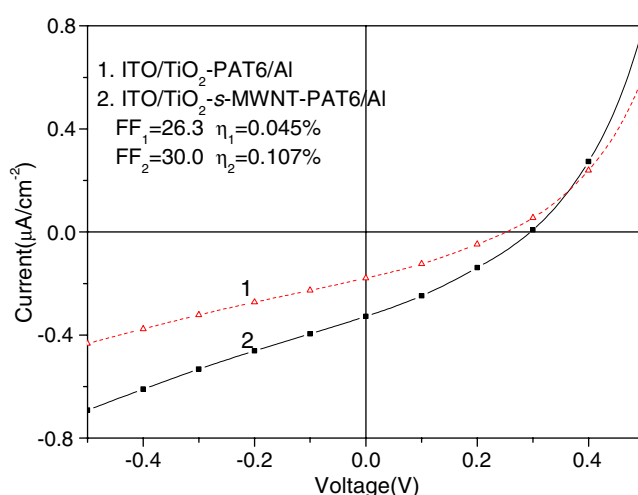


**Figure 7.** The current–voltage characteristics under illumination comparing ITO/TiO<sub>2</sub>-s-MWNT-PAT6/Al and ITO/TiO<sub>2</sub>-PAT6/Al devices.

to act as hole scavengers and charge transfer from nanotube to TiO<sub>2</sub> in the composite system of TiO<sub>2</sub> and s-MWNTs.

For the TiO<sub>2</sub>-s-MWNT we can then expect a bigger photocurrent than that of the TiO<sub>2</sub> cell since its semiconductivity ( $E_g$ ) is lower than that of TiO<sub>2</sub>, as evidenced in the UV–vis spectrum. The photoefficiency depends on both the energy required to excite the electrons from the valence band to conductivity band and the electron–hole pair recombination. In our opinion a combined effect, electron trap species, which diminishes the rate of electron pair recombination, and a lowest  $E_g$  seems to operate in the TiO<sub>2</sub>-s-MWNT composite film. The photovoltaic effect of the titania–carbon nanotube composite films has been studied and compared with that of titania. Figure 6 shows the photocurrent spectra of the devices of ITO/TiO<sub>2</sub>-PAT6/Al and ITO/TiO<sub>2</sub>-s-MWNT-PAT6/Al under illumination by a 500 W xenon lamp.

A comparative results show that the device from the TiO<sub>2</sub>-s-MWNT film exhibits better performance with regards to photocurrent than that from the TiO<sub>2</sub> film throughout nearly all of the visible wavelength range. The photocurrent from the TiO<sub>2</sub>-s-MWNT device is approximately twice that from the TiO<sub>2</sub> device. Such behaviour suggests that the incorporation of carbon nanotubes may promote forward electron transfer through the TiO<sub>2</sub>-s-MWNT film, most likely due to the introduction of conducting paths in TiO<sub>2</sub>. The existence of s-MWNTs can make the separation of holes and electrons more efficient. The charge separation of the excitons occurs at the interface not only between PAT6 and TiO<sub>2</sub> but also between s-MWNTs and TiO<sub>2</sub>. Both the absorption spectra and photocurrent spectra suggest that the s-MWNT is the photoactive species and the photoelectrical properties of TiO<sub>2</sub> can be greatly improved by the assembly process.

The current–voltage characteristics of the devices under illumination are shown in figure 7. All devices are irradiated with the light of 600 nm and  $27 \mu\text{W cm}^{-2}$  in intensity from the side of the ITO electrode. Fill factor (FF) [26] is defined as  $FF = I_{\text{max}} V_{\text{max}} / I_{\text{sc}} V_{\text{oc}}$ . Conversion efficiency ( $\eta$ ) is defined as  $\eta = I_{\text{sc}} \times V_{\text{oc}} \times FF / P_{\text{opt}}(\lambda)$ , where  $I_{\text{max}}$ ,  $V_{\text{max}}$ ,  $I_{\text{sc}}$ ,  $V_{\text{oc}}$  and  $P_{\text{opt}}(\lambda)$  are the current and voltage values for the maximum power point in the  $I$ – $V$  curve under illumination, the short circuit, open circuit voltage and incident light flux in  $\text{W cm}^{-2}$ ,



respectively. The single layer sandwiched between an ITO and Al electrodes exhibited a rectifying behaviour, characteristic of a Schottky diode at the junction. A nearly twofold increase in the conversion efficiency of the ITO/TiO<sub>2</sub>-s-MWNT-PAT6/Al device over that of the ITO/TiO<sub>2</sub>-PAT6/Al device was obtained owing to the increase of the effective interface area.

#### 4. Conclusions

The present results demonstrate the evident enhancement of interfacial electron separation and transfer by s-MWNT that is coated by TiO<sub>2</sub> particles. Some of the novel properties can be revealed in the formation of new nanocomposites owing to the s-MWNT coated by TiO<sub>2</sub> particles, such as morphology, absorption, luminescence and photoconductivity. Such composites are expected to be useful for applications as diverse as molecular electronics, photocatalysis and solar energy conversion.

#### Acknowledgments

The authors are grateful to the National Natural Science Foundation of China (No 60307001) and the Natural Science Foundation of Tianjin City for financial support.

#### References

- [1] Fujii A, Zakhidov A, Borovkov V, Ohmori Y and Yoshino K 1996 *Japan. J. Appl. Phys.* **35** L1438
- [2] Tada K, Onoda M, Nakayama H and Yoshino K 1999 *Synth. Met.* **102** 982
- [3] Harrison M G and Gruner J 1997 *Synth. Met.* **84** 653
- [4] Sarciftci N S, Braun D, Zhang C, Srdanov V Z, Heeger A J, Stucky G and Wudl F 1993 *Appl. Phys. Lett.* **62** 585
- [5] Yoshino K, Yin X H, Muro K, Kiyomatsu S, Morita S, Zakhidov A A, Noguchi T and Ohnishi T 1993 *Japan. J. Appl. Phys.* **32** L357
- [6] Kalls J J M, Pichler K, Friend R H, Moratti S C and Holmes A B 1996 *Appl. Phys. Lett.* **68** 3120
- [7] Kymakis E and Amaratunga G A J 2002 *Appl. Phys. Lett.* **80** 112
- [8] Ago H, Petritsch K, Shaffer M S P, Windle A H and Friend R H 1999 *Adv. Mater.* **11** 1281
- [9] Regan B O' and Gratzel M 1991 *Nature* **303** 737
- [10] Nazeeruddin M K, Kay A, Rodicio I, Humphry-Baker R, Muller E, Liska P, Vlachopoulos P N and Gratzel M 1993 *J. Am. Chem. Soc.* **115** 6382
- [11] Banerjee S and Wong S S 2002 *Nano Lett.* **2** 195
- [12] Jung K, Hong J S, Vittal R and Kim K 2002 *Chem. Lett.* **31** 864
- [13] Jitianu A, Cacciaguerra T, Benoit R, Delpeux S, Béguin F and Bonnamy S 2004 *Carbon* **42** 1147
- [14] Jitianu A, Cacciaguerra T, Berger M, Benoit R, Béguin F and Bonnamy S 2004 *J. Non-Cryst. Solids* **345/346** 596
- [15] Sainsbury T and Fitzmaurice D 2004 *Chem. Mater.* **16** 3780
- [16] Jang S R, Vittal R and Kim K J 2004 *Langmuir* **20** 9807
- [17] Kovtyukhova N I and Mallouk T E 2005 *Adv. Mater.* **17** 187
- [18] Feng W, Zhou F, Wang X, Wan M, Fujii A and Yoshino K 2003 *Chin. Phys. Lett.* **20** 753
- [19] Sugimoto R, Takeda S, Gu H B G and Yoshino K 1986 *Chem. Express* **1** 870
- [20] Lawless D, Kapoor S and Meisel D 1995 *J. Phys. Chem.* **99** 10329
- [21] Guan K and Yin Y 2005 *Mater. Chem. Phys.* **92** 10
- [22] Biniak S, Szymanski G, Siedlewski J and Swiatkowski A 1997 *Carbon* **35** 1799
- [23] Yang R T, Li W B and Chen N 1998 *Appl. Catal. A* **169** 215
- [24] Riggs J E, Guo Z, Carroll D L and Sun Y 2000 *J. Am. Chem. Soc.* **122** 5879
- [25] Kymakisa E and Amaratunga G A J 2002 *Appl. Phys. Lett.* **80** 112
- [26] Brabec C J N, Sariciftci S and Hummelen J C 2001 *Adv. Funct. Mater.* **11** 15